Chemical Engineering Journal 354 (2018) 35–41

Contents lists available at ScienceDirect

Chemical Engineering Journal

journal homepage: www.elsevier.com/locate/cej

Tube-in-tube hollow fiber catalytic membrane microreactor for the hydrogenation of nitrobenzene

Ming Liu[a,b], Xun Zhu[a,b,*], Rong Chen[a,b], Qiang Liao[a,b], Dingding Ye[a,b], Biao Zhang[a,b], Jian Liu[a,b], Gang Chen[a,b], Kun Wang[a,b]

[a] Key Laboratory of Low-Grade Energy Utilization Technologies and Systems (Chongqing University), Ministry of Education, Chongqing 400030, China
[b] Institute of Engineering Thermophysics, Chongqing University, Chongqing 400030, China

HIGHLIGHTS

- A tube-in-tube hollow fiber catalytic membrane microreactor was developed.
- Hollow fiber catalytic membrane was formed by the layer-by-layer self-assembly method.
- The developed catalytic membrane showed good activity and mass transfer efficiency.
- Good performance and stability were achieved by the developed membrane microreactor.

ARTICLE INFO

Keywords:
Hollow fiber catalytic membrane
Membrane microreactor
Layer-by-layer self-assembly
Polydopmine modification
Nitrobenzene conversion

ABSTRACT

The miniaturization of membrane reactors aims to improve the mass transfer efficiency. A tube-in-tube hollow fiber catalytic membrane microreactor that contains dual characteristics of a catalytic membrane reactor and a microreactor was developed in this study. For a gas-liquid-solid (G-L-S) reactor, the immobilization of solid catalysts on a hollow fiber membrane (HFM) via layer-by-layer (LBL) self-assembly enables the model reaction of nitrobenzene hydrogenation to occur. The unique structure of the novel catalytic membrane microreactor separates the gas and liquid reactants and shortens the transfer distance. The experimental results showed that the nitrobenzene conversion was high during 30 h of continuous operation. The effects of the flow rates and inlet nitrobenzene concentration were also investigated. At a given gas flow rate, the nitrobenzene conversion and concentration of the product aniline decreased with increasing the liquid flow rate. Meanwhile, at a given liquid flow rate, an increase in the gas flow rate led to an increase in the pressure of the gas phase. Sufficient hydrogen promoted the reaction, increasing the nitrobenzene conversion and aniline concentration. In addition, the inlet nitrobenzene concentration affected the conversion. Higher concentration not only enhanced the reaction rate but also caused catalyst poisoning. Based on these results, the newly designed catalytic membrane microreactor is feasible to improve the performance towards multiphase reaction.

1. Introduction

Membrane reactors have undergone rapid development because their unique structure can efficiently separate the different phases of the system. As a result, membrane reactors have been widely utilized in many applications, such as separation [1], pervaporation [2], distillation [3], catalysis [4] and multiphase reactions [5]. In particular, because membrane reactors can simultaneously generate and separate products and have a membrane structure that provides an extensive contact area between different phases, the application of membrane reactors in multiphase reactions has been very popular and received considerable attention. Typically, a membrane reactor for a three-phase catalytic reaction allows liquid and gas streams to contact each other via a membrane with a catalyst deposited on its surface. The liquid and gas reactants have to diffuse to the catalytic surface in order to react with each other. Diffusion, as the main transfer mode in membrane reactors, has a significant effect on the reaction rate. Shortening the transfer paths of different reactants is beneficial for the diffusion and improving the reaction rates. Therefore, ways to provide a shorter transfer path and improve the reaction rate are important areas of

* Corresponding author at: Key Laboratory of Low-Grade Energy Utilization Technologies and Systems (Chongqing University), Ministry of Education, Chongqing 400030, China.
E-mail address: zhuxun@cqu.edu.cn (X. Zhu).

https://doi.org/10.1016/j.cej.2018.07.203
Received 9 May 2018; Received in revised form 11 July 2018; Accepted 29 July 2018
Available online 30 July 2018
1385-8947/

research. Narrowing the spaces on both sides of the membrane can shorten the transfer distance and improve the catalytic reaction rate. From this point of view, the miniaturization of membrane reactors is a promising way to improve their performances.

Among the numerous membrane materials, hollow fiber modules might be the most compact configuration with a very high packing density and a diameter of a few millimeters. Unlike other membranes, the specific surface area of a hollow fiber is very high and can reach 30,000 m^2/m^3. Therefore, a hollow fiber membrane (HFM) can be considered as a microchannel with a high specific surface area and a short diffusion path [6] and is able to separate and infiltrate different phases [7,8]. In addition, hollow fiber substrates possess several advantages for fabricating membrane microreactors, such as easy scale-up and catalyst loading [9,10]. In this case, metal nanoparticles are uniquely superior catalysts with a high surface area-to-volume ratio can be easily immobilized on hollow fiber membranes. Metal nanoparticles are typically prepared by impregnation, in-situ reduction or chemical vapor deposition [11,12]. However, the particles prepared using these methods are frequently non-uniform and easily leached. To cope with these issues, the layer-by-layer (LBL) self-assembly deposition of polycations and polyanions ensures that catalytic nanoparticles are immobilized on HFMs. The selective adsorption of oppositely charged polyelectrolytes provides a simply way to deposit a controllable support film for metal nanoparticles. In 1942, Decher [13] first came up with this versatile method that enabled the construction of functional multilayer films. The electrostatic attraction between the polyelectrolyte components is the principal driving force of the LBL self-assembly, but covalent bonding [14], hydrogen bonding [15], hydrophobic interactions [16] and charge transfer [17] are also associative interactions. Kidambi et al. [18] investigated the LBL deposition of a polyelectrolyte on alumina and the subsequent reduction of Pd^{2+} as a versatile method for synthesizing immobilized Pd nanocatalysts. Kaner et al. [19] successfully modified a commercial polyethersulfone membrane by an LBL self-assembly method to prevent extensive organic and biological fouling and improve water permeability. Ouyang et al. [20] investigated metal nanoparticles immobilized on HFMs via a polyelectrolyte and negatively charged Au nanoparticles. Macanas et al. [21] prepared polymer-stabilized metal nanoparticles in a functionalized polymeric membrane by polyelectrolyte deposition. These studies have paved the way for manufacturing an efficient catalyst layer by adhering polyelectrolyte multilayers (PEMs). Although numerous studies have been carried out, the chemical performance and stability of hollow fibers is unsatisfied. Dopamine exhibits very robust and strong adhesion, acting as a multifunctional material to increase stability [22–24]. In this study, a polydopamine (PDA) film was coated on a hollow fiber prior to introducing the PEMs. A literature review indicated that the catechol group in dopamine can adhere to many types of surfaces because of its mussel-mimicking versatility. PEMs can deposit on a HFM via hydrophobic interactions [25]. The PDA pretreatment make the HFM more stable for the catalyst loading because of the above characteristics.

This paper describes an autonomous tube-in-tube hollow fiber catalytic membrane microreactor consisting of a modified HFM and a polytetrafluoroethylene (PTFE) capillary with the aim of improving the mass transfer and reaction rate. The tube-in-tube design provides a large contact area between gas and liquid reactants and a region for catalyst loading. Coating the HFM with a catalyst layer enables the miniaturization of the membrane reactor, and this structure combines the merits of membrane and microreactor technologies. Thus, a novel device with a large surface-area-to-volume ratio, short transfer distance, and excellent flexibility was created. All of these characteristics are especially profitable for gas-liquid-solid (G-L-S) catalytic reactions. This work took advantage of the device to investigate the performance of the reaction about hydrogenation of nitrobenzene. A catalyst layer of Pd nanoparticles was coated on a single hollow fiber, which was modified by LBL self-assembly. An additional layer of PDA film can effectively improve the stability of the catalytic membrane microreactor. Some of the critical parameters (i.e., PDA film, gas flow rate, liquid flow rate and inlet nitrobenzene concentration) of the hollow fiber catalytic membrane microreactor were investigated to optimize the microreactor design. The feasibility of this design will be useful for the development of membrane microreactors.

2. Experimental section

2.1. Chemicals and materials

In this work, dopamine hydrochloride, nitrobenzene and $NaBH_4$ were purchased from Aladdin Industrial Inc. (Shanghai, China). Tris (hydroxymethyl) aminomethane was obtained from GEN-VIEW Scientific Inc. (Florida, USA). Palladium chloride was obtained from Sino-Platinum Metals Co. Ltd. (Kunming, China). Ethanol and NaCl were acquired from Chongqing Chuandong Chemical Co. Ltd. (Chongqing, China). Poly(sodium 4-styrenesulfonate) (PSS, Mw = 70,000) and poly(allylamine hydrochloride) (PAH, Mw = 17,500) were supplied by Sigma-Aldrich (Shanghai, China). Deionized water was used in the experiments in the reactant solutions and for rinsing and the preparation of dopamine and the polyelectrolyte, which was obtained from an Ultrapure water system (ROMB, Chongqing, China). The pH of the polyelectrolytes was adjusted by dilute HCl or NaOH. All chemicals were used as received. A polypropylene (PP) hollow fiber used as the membrane was supplied by the Haotian Co. (Hangzhou, China). The inner diameter of the hollow fiber was 350 μm, the thickness was 100 μm, and the effective length was 0.5 m. A PTFE capillary tube with an inner diameter of 1.0 mm was used as the external annular tube to hold the hollow fiber catalytic membrane.

2.2. Preparation of the hollow fiber catalytic membrane

In this study, the hollow fiber catalytic membrane was formed by coating the hollow fiber with a palladium nanoparticle catalyst layer. The preparation of the catalyst layer on the hollow fiber was realized by the LBL self-assembly method. The HFM was built in a capillary tube in order to achieve the modifications. The modification process generally involves directly immersing the hollow fibers in polyelectrolyte solutions. However, the extent of conversion and time required were unsatisfactory. In this work, hence, dopamine was first deposited on the surface of the hollow fiber to form a PDA film as an adhesive for polyelectrolyte solutions that would previously pass through the fiber. PDA has many significant advantages, especially its adhesive property. PDA can bind hollow fibers together in a manner similar to the adhesive action of mussels. Additionally, PDA is zwitterionic due to its diverse functional groups such as catechol and amino groups. Below pH = 4, the amino groups are protonated, and the dopamine surface carries positive charges [25]. To do this, the hollow fiber was first rinsed with deionized water for 30 min to remove impurities. Then, an aqueous dopamine solution was passed through the fiber, and a PDA coating was formed on the fiber surface. The aqueous dopamine solution composed of 2 mg of dopamine per milliliter and 10 mM tris(hydroxymethyl) aminomethane was pumped into the HFM at a flow rate of 20 μL/min for 6 h. Then, the solution was removed from the module by rinsing with deionized water and drying at 65 °C for 1 h under nitrogen environment. The dopamine self-polymerization formed a PDA film adhered to the hollow fiber, and the color of the hollow fiber changed from white to brown. After the deposition of the PDA film, the PEMs were prepared by alternating adsorption of polycations and polyanions. First, a dilute aqueous containing 0.02 M PSS and 0.5 M NaCl solution was fed into the module at a flow rate of 40 μL/min for 1 h, followed by rinsing with deionized water at the same flow rate for 0.5 h to remove excess polyelectrolytes. As mentioned above, the amino groups of PDA will be protonated below pH = 4. Therefore, the PSS solution was adjusted to pH 3.5 using NaOH or HCl to allow the polyanion to combine

with the PDA coating. Subsequently, a polycationic solution containing 0.02 M PAH and 0.5 M NaCl was pumped into the module at a flow rate of 40 μL/min for 1 h, followed by rinsing with deionized water at the same flow rate for 0.5 h. Hence, the oppositely charged polyelectrolytes were deposited on the fiber through electrostatic interactions. This polyelectrolyte deposition process was repeated 4 times to obtain abundant charge carriers, which improve the catalyst loading. Next, a palladium chloride solution was prepared in HCl (10 mM) and injected via syringe into the module at a flow rate of 10 μL/min for 3 h. For palladium reduction, a dilute aqueous $NaBH_4$ solution (10 mM) passed through the fiber for 2 h at a flow rate of 10 μL/min in an ice bath. The module was washed with deionized water and dried under nitrogen environment. The hollow fiber catalytic membrane was extracted from the capillary tube for fabrication of the membrane microreactor. In consideration of this fabrication, the catalyst layer on the HFM was prepared with three coatings: a PDA film, PEM and reduced palladium catalytic membrane.

2.3. Fabrication of the tube-in-tube hollow fiber catalytic membrane microreactor

The tube-in-tube hollow fiber catalytic membrane microreactor contained an internal hollow fiber catalytic membrane and external PTFE capillary tube. To permit the gaseous and liquid streams to flow into the membrane microreactor at the same time, an autonomous connector with two exits made by a syringe needle was adopted in the experiment. As illustrated in Fig. 1, the catalyst coated HFM was placed into a PTFE capillary. At the entrance of the tube, there was a specialized needle connected to the both the capillary tube and hollow fiber. Every capillary tube in this study included only one hollow fiber that allowed for gas flow. The middle interval between the hollow fiber and capillary tube was the passageway for the liquid reactant. The microchannel for gas flow had a volume of 48 μL, a length of 50 cm and a diameter of 350 μm. The external microchannel for the liquid reactant had a volume of 474.9 μL, an outer diameter of 1 mm, an inner diameter of 450 μm and a length of 50 cm.

2.4. Experimental setup

The catalytic performance of the developed tube-in-tube HFM microreactor was evaluated by a G-L-S (three-phase) model reaction, the hydrogenation of nitrobenzene on palladium nanoparticles. Fig. 2 shows a diagram of the experimental system. Nitrobenzene was dissolved in ethanol:water (7:3 by volume) and supplied as the liquid reactant, which was pumped into the PTFE capillary using a syringe pump (Longer, China). Hydrogen was fed into the HFM, and the flow rate was controlled by a mass flow meter (Omega, USA). The reaction was conducted at room temperature. The reactant nitrobenzene and the desired product aniline were contained in the liquid phase and collected at the outlet. The concentrations of these compounds were measured by a gas chromatograph (7890B, Agilent, USA) equipped with a flame

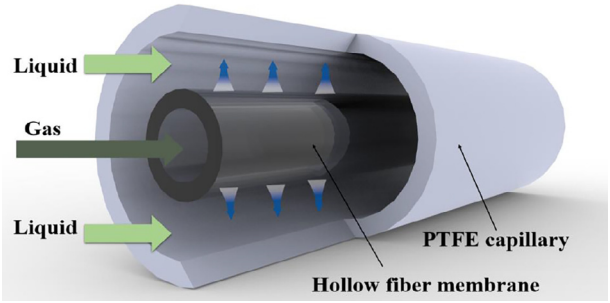

Fig. 1. Schematic of the tube-in-tube hollow fiber catalytic membrane microreactor.

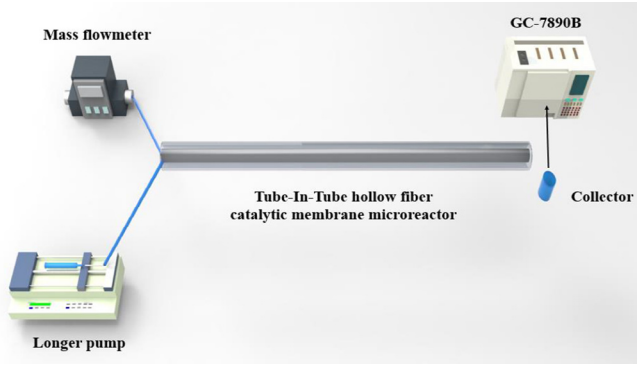

Fig. 2. Schematic of the experimental setup.

ionization detector (FID). Since one mole of nitrobenzene can theoretically produce one mole of aniline, the nitrobenzene conversion efficiency can be calculated from the ratio of the aniline concentration at the outlet to the nitrobenzene concentration at the inlet.

3. Results and discussion

3.1. Materials characterization

3.1.1. Textural characterization

The surface morphology of the modified HFM was characterized by SEM (JSM-7800F). Since the hollow fiber is insulated and the adsorption of the films occurs on both the internal and external surfaces of the fibers, the surfaces of the membrane were sputtered with gold before the test. Fig. 3a shows the SEM images of the internal and external surfaces of the original HFM. The hollow fiber had a homogeneous mesh structure both inside and outside. After deposition of the PDA film, the morphology of the hollow fiber almost remained unchanged, as depicted in Fig. 3b. Sufficient membrane pores existed on both the internal and external surfaces, and the pore sizes were uniform. PEMs were then formed on the PDA surface, which was accompanied by pore blockage. The results presented in Fig. 3c demonstrate that the PEMs covered the fiber and altered the morphological features. With the reduction of the catalyst, catalyst nanoparticles appeared on the surface of the hollow fiber. Uniform Pd nanoparticles were well separated with no apparent aggregation, and the particle size was below 100 nm (Fig. 3d). These results demonstrate that the HFM was modified with the PDA/PSS/PAH/Pd films.

3.1.2. Characterization of the Pd nanocatalyst

X-ray photoelectron spectroscopy (XPS) analysis was performed in order to evaluate the chemical compositions of the surfaces of the original and modified HFMs. The measurements were carried out using an ESCALAB 250Xi XPS system (Thermo, USA) with monochromatic and focused Al Kα radiation ($h\nu = 1486.6$ eV) delivered at a power of 150 W. Fig. 4 shows different spectra acquired over a range of 250–450 eV. The spectrum of the raw hollow fiber contained only one peak corresponding to C 1 s. After the PDA layer had formed, an N 1 s peak appeared. Other than the S 2 s peak, no peaks of Pd were found in the spectrum of the hollow fiber with PDA and PEMs, which implies that PSS had adsorbed on the PDA coating. In addition, the characteristic N 1 s peak was larger in the green spectrum than in the pink spectrum, illustrating a higher nitrogen content in PDA (PSS/PAH) than that in PDA. After the reduction of $PdCl_4^{2-}$ complex ions, two additional peaks corresponding to $Pd^0(3d_{5/2})$ and $Pd^0(3d_{3/2})$ were observed. Compared with the other three spectra, the red spectrum demonstrates that the Pd nanocatalyst was deposited on the surface of the PEMs. These results demonstrate that elemental Pd was successfully reduced and grafted on the surface of the HFM after modification with the PDA and PEMs layers.

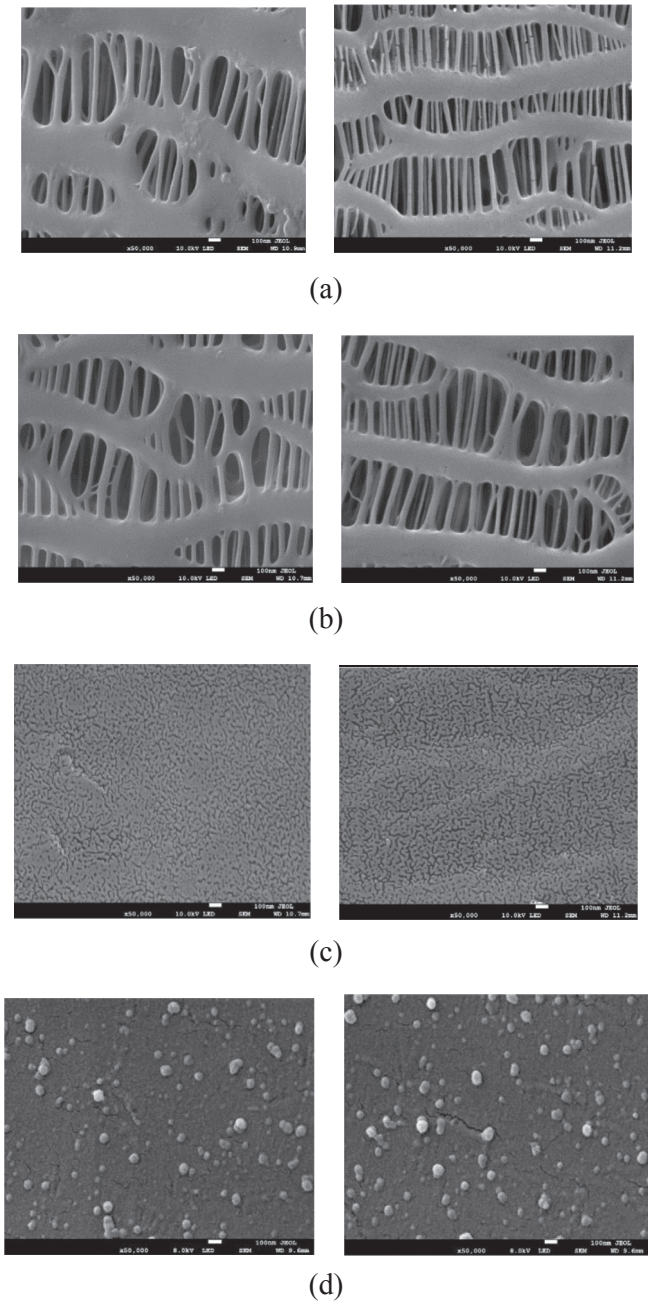

Fig. 3. SEM images of the hollow fiber catalytic membrane: (a) HFM; (b) HFM/PDA; (c) HFM/PDA/(PSS/PAH); (d) HFM/PDA/(PSS/PAH)/Pd.

To evaluate the adsorption of $PdCl_4^{2-}$ with different modifications, different concentrations of H_2PdCl_4 solutions were confirmed by UV-visible spectroscopy (T6-1650E, Persee, China) before and after adsorption. The results are shown in Fig. 5. The spectrum of the original H_2PdCl_4 solution contained a distinct peak at approximately 425 nm, which indicated the existence of $PdCl_4^{2-}$ [26]. The other spectra correspond to H_2PdCl_4 solutions that underwent different modifications. For the PDA solution, the peak corresponding to $PdCl_4^{2-}$ ions was decreased due to the adsorption by PDA. Some $PdCl_4^{2-}$ ions may have been adsorbed by the PDA layer. To determine the adsorption of the PEMs, PEM solutions were pumped into a raw hollow fiber using the same method, and the absorbance of the $PdCl_4^{2-}$ peak decreased more than with the hollow fiber modified only by PDA. This means that $PdCl_4^{2-}$ ions adsorbed to the fiber with a grafted PEM layer more than to the fiber with a PDA layer. The $PdCl_4^{2-}$ peak of the hollow fiber

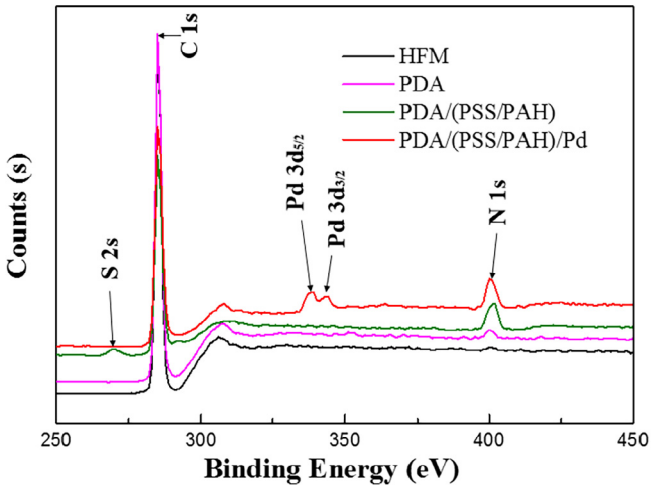

Fig. 4. XPS spectra of the HFM, PDA, PDA/(PSS/PAH) and PDA/(PSS/PAH)/Pd.

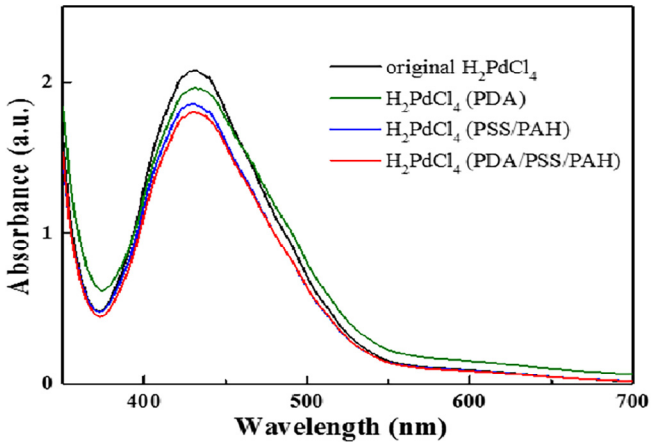

Fig. 5. UV-vis spectra of H_2PdCl_4 before and after adsorption on PDA, PSS/PAH and PDA/(PSS/PAH).

successively grafted with a PDA layer and a PEM layer was the smallest, demonstrating that the adsorption was maximal. In summary, the PDA and PEM coatings adsorbed different levels of $PdCl_4^{2-}$ ions. The amount of $PdCl_4^{2-}$ ions grafted on the PDA/PEM layers was higher than that only on the PDA coating.

3.2. Performance evaluation of tube-in-tube hollow fiber catalytic membrane microreactor

In this work, the hydrogenation of nitrobenzene catalyzed by Pd nanocatalyst served as a model reaction for examining the performance of the developed membrane microreactor. This reaction is attractive because it does not proceed in the absence of catalyst and it produces fewer byproducts. During the operation, high-purity hydrogen was fed into the interior of the modified hollow fiber while a freshly prepared aqueous ethanol solution containing 30 mM nitrobenzene flowed through the external capillary tube. After the reaction was stable, the samples were collected at the exit every 1 h. According to the above description, a complete catalyst layer coated on the membrane microreactor consisted of a PDA film, PEM film and nanocatalyst Pd. To evaluate the influence of each step, multiple tube-in-tube hollow fiber catalytic membrane microreactors with the same structure and size were fabricated. In all of these tests, the experimental conditions were the same. The hydrogen and nitrobenzene flow rates were 0.05 sccm and 10 μL/min, respectively.

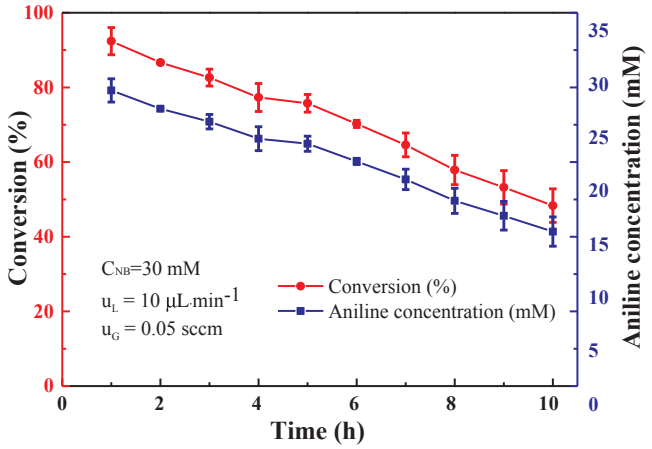

Fig. 6. Performance of the tube-in-tube hollow fiber catalytic membrane microreactor without PDA modification. Gas flow rate: 0.05 sccm; liquid flow rate: 10 μL/min; nitrobenzene concentration: 30 mM.

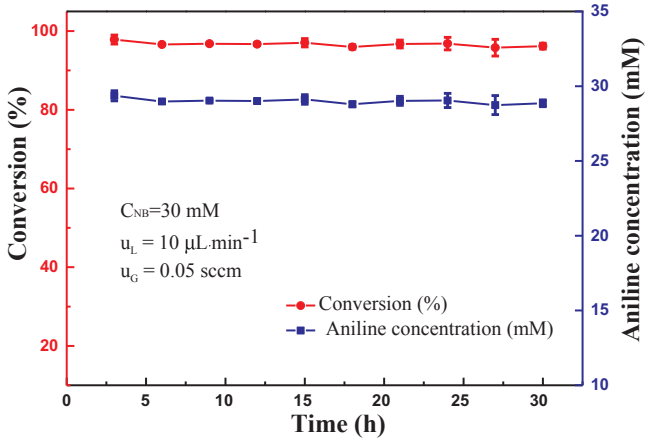

Fig. 7. Long-term performance of the tube-in-tube hollow fiber catalytic membrane microreactor. Gas flow rate: 0.05 sccm; liquid flow rate: 10 μL/min; nitrobenzene concentration: 30 mM.

An unmodified raw hollow fiber was directly used to adsorb a 10 mM H_2PdCl_4 solution. After reduction by $NaBH_4$, nitrobenzene and hydrogen were pumped into the catalytic membrane microreactor, but it was found that the solution at the outlet did not contain aniline. Therefore, no reaction had occurred between nitrobenzene and hydrogen. This fact indicated that a raw HFM was unable to adsorb $PdCl_4^{2-}$ ions. Hence, it is necessary to introduce modifications to promote the catalytic reaction. Since PSS can deposit on the HFM due to hydrophobic interactions, PSS and PAH solutions were alternately passed through a raw hollow fiber module without PDA solution. Therefore, the hollow fiber catalytic membrane was coated only with the PEMs and Pd nanocatalyst. Fig. 6 shows the aniline concentration and nitrobenzene conversion. The measured nitrobenzene conversion first remained at approximately 92% and then gradually decreased. Different from an original membrane, the HFM with PEMs could be successfully coated with Pd nanoparticles. Over 10 h of operation, the nitrobenzene conversion by the HFM with PEMs gradually decreased to 48%, and the concentration of aniline at the exit decreased to 14.5 mM. Even though the initial adsorption occurs through hydrophobic interactions between PSS and the HFM, the subsequent driving force of adsorption is the electrostatic force between negatively charged PSS and positively charged PAH. Regarding the PSS/PAH/Pd films, the presence of PSS/PAH in the films can enhance the surface charge in order to adsorb more $PdCl_4^{2-}$ ions. As the number of PEMs films increased, the active adsorption sites increased, which can adsorb more $PdCl_4^{2-}$ ions. The initial high conversion revealed that the microreactor had a good design and catalyst activity. The conversion was reduced by half after 10 h, which may have been attributed to an insufficient amount of nanocatalyst and the presence of by-products that block the catalytic sites. Another possible reason for the conversion decline may be the hydrophobic interactions. According to ICP-OES measurements (Agilent 7500ce), the Pd loading on the HFM before the reaction was 56.652 μg. After 10 h, the Pd loading decreased to 47.342 μg. Therefore, Pd leaching is a likely cause of the conversion decline in this experiment. In summary, analysis of the reaction with PSS/PAH/Pd films demonstrated that the hollow fiber catalytic membrane microreactor needs modifications to enhance the binding force between the hollow fiber surface and PEMs.

To improve the stability and conversion of the microreactor, a microreactor with a membrane that had been coated with a PDA film prior to coating with PEMs was tested. The effect of PDA/PSS/PAH/Pd films were evaluated using the same tube-in-tube structure. Fig. 7 shows the nitrobenzene conversion and aniline concentration at the exit over the entire measurement period. The conversion remained at more than 90% over 30 h of operation, and the aniline concentration exceeded 27 mM at all time. A comparison of Figs. 6 and 7 reveals that the stability and conversion of the catalytic membrane microreactor composed of PDA/PEMs/Pd were much better than those of the reactor composed of only PEMs/Pd, and this difference can be attributed to several reasons. During the modification, the PDA film adhered to the HFM prior to the PEMs. Based on previous literature, PDA can bond with many materials through functional groups such as catechol, amino and phenolic groups [25]. Catechol groups play an important role in the tight adhesion of many different structures. In addition, PDA is zwitterionic and can be grafted with polyelectrolytes through electrostatic interactions depending on its surroundings. When the pH of the PSS solution was adjusted to 3.5, the PDA surface was positively charged, and the PSS solution was negatively charged. The PDA film and PEMs film can adsorb $PdCl_4^{2-}$ ions, so that the addition of PDA film resulted in more adsorbed Pd, as illustrated in Fig. 5. More catalyst promotes the reaction to a greater extent. The above results indicate that the HFM modified by PDA and PEMs yielded a better and stable performance than other HFM based membrane microreactors, and the subsequent optimization of the reactor parameters was carried out using this modification.

To test the influence of PDA, an HFM through which PDA solution had passed for only 6 h was examined. Nitrobenzene and hydrogen flowed through an identical membrane microreactor with the same design. This comparison revealed that the PDA film can also adsorb $PdCl_4^{2-}$ ions and that the hydrogenation reaction can occur. However, the nitrobenzene conversion and stability were worse than those of an HFM coated with only PEMs/Pd. PDA can bond with metal ions through functional groups, enabling PDA to adsorb some $PdCl_4^{2-}$ ions, which allowed reaction occurred. Nevertheless, the performance of this system was poor. Fig. 3b shows that the morphology of the HFM remained unchanged, similar to that of a raw HFM. Therefore, the PDA film adsorbed on only the network structure of original HFM. The UV-visible spectra also indicated that the PDA film adsorbed the smallest amount of $PdCl_4^{2-}$ ions. Overall, these results indicate that PDA can promote the reaction, but modification with only a PDA film is not sufficient to adsorb $PdCl_4^{2-}$ ions and thereby promote the reaction.

3.3. Effect of the liquid flow rate

In this experiment, the liquid flow rate was varied, and the mass transfer of the microreactor was investigated. The gas flow rate was held at 0.05 sccm, while the flow rate of feeding solution ranged from 10 μL/min to 80 μL/min. The concentration of nitrobenzene at the inlet was maintained at 50 mM. Fig. 8 shows that the conversion of nitrobenzene and the product concentration decreased with increasing

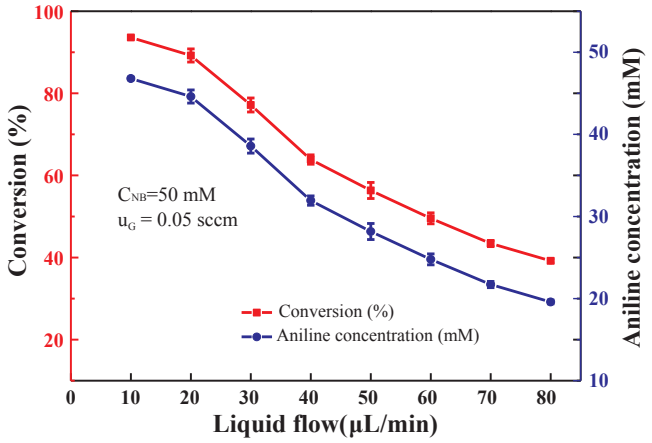

Fig. 8. Effect of the liquid flow rate on the nitrobenzene conversion. Gas flow rate: 0.05 sccm; nitrobenzene concentration: 50 mM.

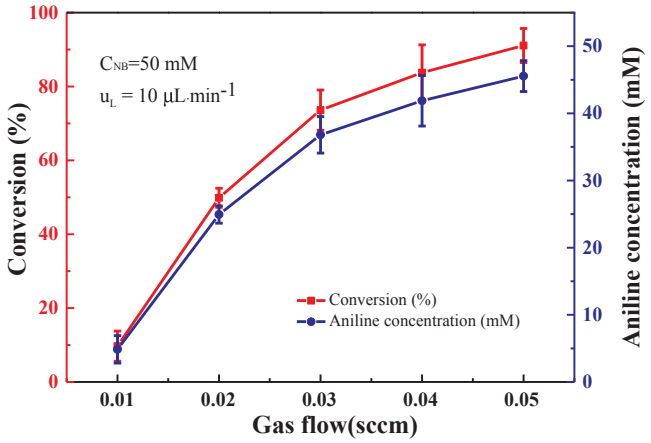

Fig. 9. Effect of the gas flow rate on the nitrobenzene conversion. Liquid flow rate: 10 μL/min; nitrobenzene concentration: 50 mM.

the liquid flow rate. For a given gas flow rate, the reaction initially resulted in a conversion of more than 93% at a relatively low liquid flow rate. Hence, it can be speculated that the supplied hydrogen reacted completely with the nitrobenzene solution. With an increases in the liquid flow rate, the residence time gradually decreased. Hence, the effective reaction time of nitrobenzene was also reduced when the flow rate was increased to 80 μL/min. Too high liquid flow rate directly resulted in partial discharge of the nitrobenzene fed from the membrane microreactor without reaction, and the product aniline was diluted by the increased volume of feed solution. On the other hand, the increase of the liquid flow rate increased the pressure in the capillary, and because the pressure on the gas side remained the same, the gas compartment was compressed by the liquid compartment. Therefore, the hydrogen concentration of the catalyst layer was gradually reduced, and the mass transport resistance of hydrogen increased. Both the reaction rate and time decreased such that the conversion of nitrobenzene and the aniline concentration clearly decreased. In summary, the liquid flow rate can greatly affect the reaction rate and time. With increasing the liquid flow rate, the nitrobenzene conversion and aniline concentration decrease.

3.4. Effect of the gas flow rate

The gaseous reactant was high-purity hydrogen, and it had an important effect on the conversion of nitrobenzene and the aniline product. In this experiment, the liquid flow rate was maintained at 10 μL/min, and the inlet nitrobenzene concentration was kept at 50 mM. The only variable was the gas flow rate, which was varied from 0.01 sccm to 0.05 sccm. As shown in Fig. 9, when the initial gas flow rate was 0.01 sccm, the conversion of nitrobenzene was only 9.7%. As the gas flow rate increased, the conversion continuously increased. When the gas flow rate was increased to 0.05 sccm, the conversion of nitrobenzene and the aniline concentration were 91% and 45.5 mM, respectively. These results show that the performance of the microreactor was improved by more hydrogen, which can be explained by the following reasons. Increasing the gas flow rate increased the hydrogen pressure in the HFM and caused hydrogen concentration at the catalyst layer to be increased, which increased the reaction rate. An insufficient hydrogen concentration may allow the liquid feed solution to compress the gas reactant. Correspondingly, there would be less gas available for the reaction. Increasing the gas flow rate increased the pressure, which was dramatically improved by the satisfactory permeability of the HFM. More hydrogen at the catalyst layer produced more aniline. At a given liquid flow rate, the increase in the gas flow rate increased both the conversion and product concentration. These results indicate that a relatively higher gas flow rate is required for a better performance of the catalytic membrane microreactor.

3.5. Effect of the inlet nitrobenzene concentration

In this experiment, the inlet nitrobenzene concentration was varied, and the nitrobenzene conversion and aniline concentration were investigated. The gas and liquid flow rates were kept at 0.05 sccm and 10 μL/min, respectively. The nitrobenzene concentration at the inlet was 30, 50, 70, 90 or 110 mM. Fig. 10 shows the variations of the nitrobenzene conversion and aniline concentration with the inlet nitrobenzene concentration under the same gas and liquid flow rates. As the nitrobenzene concentration increased, the conversion decreased, while the aniline concentration increased. Increasing the nitrobenzene concentration decreased the nitrobenzene conversion from 93% to 70%, but increased the aniline concentration from 27.9 mM to 77 mM. The reasons leading to these phenomena can be described as follows. The increased inlet nitrobenzene conversion could enhance the catalytic reaction, which would also produce more aniline. However, the catalytic capacity of the microreactor was limited. The high concentration of nitrobenzene in solution could more easily lead to catalyst poisoning, which would generate more byproducts such as nitrotoluene and nitrosobenzene. Thereby, the nitrobenzene conversion would decrease with the increasing nitrobenzene concentration. Based on these results, it can be concluded that a low inlet nitrobenzene concentration benefitted the product concentration but not the nitrobenzene conversion. However, the nitrobenzene conversion was maintained at a higher

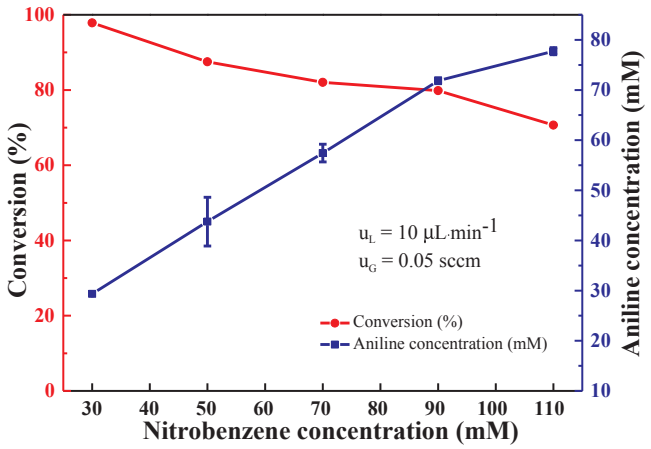

Fig. 10. Effect of the inlet nitrobenzene concentration on the nitrobenzene conversion. Liquid flow rate: 10 μL/min; gas flow rate: 0.05 sccm.

level and did not dramatically decrease at an inlet nitrobenzene concentration of 110 mM, which illustrates the excellent performance of our catalytic membrane microreactor.

4. Conclusions

In this work, a novel hollow fiber catalytic membrane microreactor was successfully developed for a G-L-S reaction system using a tube-in-tube structure and LBL self-assembly. The catalytic reaction of nitrobenzene with hydrogen was used to evaluate the performance of the catalytic membrane microreactor. The tube-in-tube hollow fiber modules provided two different passages that allowed the liquid reactant to flow through the external PTFE capillary and the gas to flow through the microchannel supplied by the hollow fiber. The HFM module was modified with PDA and polyelectrolyte films. A Pd nanocatalyst layer was finally grafted on the HFM by LBL self-assembly. Because the hollow fiber had significant permeability to gas, hydrogen readily penetrated the membrane and reacted on the catalyst layer. Based on the surface topography and elemental analysis, it can be concluded that the catalytic nanoparticles were successfully deposited and well distributed on the HFM. Varying the reactor parameters revealed the effects of different modifications, the liquid flow rate, the gas flow rate and the inlet nitrobenzene concentration on the reactor performance. The microreactor performed well in a long-term test that lasted 30 h due to its unique structure and the modification of the HFM. A PDA film improved the stability of the reaction. Increasing the gas flow rate or decreasing the liquid flow rate increased the aniline concentration and nitrobenzene conversion. At given liquid and gas flow rates, the inlet nitrobenzene concentration was the key component affecting the reactor performance. Due to the limited catalytic ability of the reactor, not all the nitrobenzene was converted to aniline. A higher supplied nitrobenzene concentration corresponded to a higher aniline product concentration and a lower nitrobenzene conversion. The obtained results demonstrate that our catalytic membrane microreactor is useful for G-L-S reactions. Especially for those hydrogenation reactions and catalytic reduction, good performance can also be achieved due to the offered advantages, such as a high specific surface area and controllable catalytic interface. This new catalytic membrane microreactor design open a new window for the development of multiphase catalytic reaction systems.

Acknowledgements

The authors gratefully acknowledge the financial supports of the National Natural Science Foundation of China (No. 51620105011) and the Fundamental Research Funds for the Central Universities (No. 2018CDXYDL0001).

References

[1] S. Adhikari, S. Fernando, Hydrogen membrane separation techniques, Ind. Eng. Chem. Res. 45 (2006) 875–881.
[2] S.-L. Wee, C.-T. Tye, S. Bhatia, Membrane separation process—pervaporation through zeolite membrane, Sep. Purif. Technol. 63 (2008) 500–516.
[3] M.S. El-Bourawi, Z. Ding, R. Ma, M. Khayet, A framework for better understanding membrane distillation separation process, J. Membr. Sci. 285 (2006) 4–29.
[4] K. Georgieva, I. Mednev, D. Handtke, J. Schmidt, Influence of the operating conditions on yield and selectivity for the partial oxidation of ethane in a catalytic membrane reactor, Catal. Today 104 (2005) 168–176.
[5] M. Vospernik, A. Pintar, G. Berčič, J. Levec, J. Walmsley, H. Ræder, I.E. Emil, M. Sylvain, D. Jean-Alain, Performance of catalytic membrane reactor in multiphase reactions, Chem. Eng. Sci. 59 (2004) 5363–5372.
[6] S.-P. Yan, M.-X. Fang, W.-F. Zhang, S.-Y. Wang, Z.-K. Xu, Z.-Y. Luo, K.-F. Cen, Experimental study on the separation of CO2 from flue gas using hollow fiber membrane contactors without wetting, Fuel Process. Technol. 88 (2007) 501–511.
[7] J. Lee, H.K. Lee, K.E. Rasmussen, S. Pedersen-Bjergaard, Environmental and bioanalytical applications of hollow fiber membrane liquid-phase microextraction: a review, Anal. Chim. Acta 624 (2008) 253–268.
[8] H.A. Rangwala, Absorption of carbon dioxide into aqueous solutions using hollow fiber membrane contactors, J. Membr. Sci. 112 (1996) 229–240.
[9] S.J. Choi, M.P. Kim, S.J. Lee, B.J. Kim, I.D. Kim, Facile Au catalyst loading on the inner shell of hollow SnO2 spheres using Au-decorated block copolymer sphere templates and their selective H2S sensing characteristics, Nanoscale 6 (2014) 11898–11903.
[10] S. Dixit, R. Chinchale, S. Govalkar, S. Mukhopadhyay, K.T. Shenoy, H. Rao, S.K. Ghosh, A mathematical model for size and number scale up of hollow fiber modules for the recovery of uranium from acidic nuclear waste using the DLM technique, Separation Sci. Technol. 48 (2013) 2444–2453.
[11] J. Wagner, T. Kirner, G. Mayer, J. Albert, J.M. Köhler, Generation of metal nanoparticles in a microchannel reactor, Chem. Eng. J. 101 (2004) 251–260.
[12] J. Kim, G.Y. Han, C.-H. Chung, Encapsulating the electroluminescent phosphor micro-particles using a pulsed metal-organic chemical vapor deposition process in a fluidized bed, Thin Solid Films 409 (2002) 58–65.
[13] G. Decher, Fuzzy nanoassemblies: toward layered polymeric multicomposites, Science 277 (1997) 1232–1237.
[14] C.-J. Huang, F.-C. Chang, Using click chemistry to fabricate ultrathin thermoresponsive microcapsules through direct covalent layer-by-layer assembly, Macromolecules 42 (2009) 5155–5166.
[15] Z. Liang, O.M. Cabarcos, D.L. Allara, Q. Wang, Hydrogen-bonding-directed layer-by-layer assembly of conjugated polymers, Adv. Mater. 16 (2004) 823–827.
[16] J. Zhao, F. Pan, P. Li, C. Zhao, Z. Jiang, P. Zhang, X. Cao, Fabrication of ultrathin membrane via layer-by-layer self-assembly driven by hydrophobic interaction towards high separation performance, ACS Appl. Mater. Interfaces 5 (2013) 13275–13283.
[17] W.S. Alencar, F.N. Crespilho, M.R.M. Santos, V. Zucolotto, O.N. Oliveira, W.C. Silva, Influence of film architecture on the charge-transfer reactions of metallophthalocyanine layer-by-layer films, J. Phys. Chem. C 111 (2007) 12817–12821.
[18] S. Kidambi, J. Dai, J. Li, M.L. Bruening, Selective hydrogenation by Pd nanoparticles embedded in polyelectrolyte multilayers, J. Am. Chem. Soc. 126 (2004) 2658–2659.
[19] P. Kaner, D.J. Johnson, E. Seker, N. Hilal, S.A. Altinkaya, Layer-by-layer surface modification of polyethersulfone membranes using polyelectrolytes and AgCl/TiO2 xerogels, J. Membr. Sci. 493 (2015) 807–819.
[20] L. Ouyang, D.M. Dotzauer, S.R. Hogg, J. Macanás, J.-F. Lahitte, M.L. Bruening, Catalytic hollow fiber membranes prepared using layer-by-layer adsorption of polyelectrolytes and metal nanoparticles, Catal. Today 156 (2010) 100–106.
[21] J. Macanás, L. Ouyang, M.L. Bruening, M. Muñoz, J.C. Remigy, J.F. Lahitte, Development of polymeric hollow fiber membranes containing catalytic metal nanoparticles, Catal. Today 156 (2010) 181–186.
[22] H. Lee, S.M. Dellatore, W.M. Miller, P.B. Messersmith, Mussel-inspired surface chemistry for multifunctional coatings, Science 318 (2007) 426–430.
[23] W.-B. Tsai, C.-Y. Chien, H. Thissen, J.-Y. Lai, Dopamine-assisted immobilization of poly(ethylene imine) based polymers for control of cell–surface interactions, Acta Biomater. 7 (2011) 2518–2525.
[24] Y. Liu, K. Ai, L. Lu, Polydopamine and its derivative materials: synthesis and promising applications in energy, environmental, and biomedical fields, Chem. Rev. 114 (2014) 5057–5115.
[25] R. Malaisamy, M.L. Bruening, High-flux nanofiltration membranes prepared by adsorption of multilayer polyelectrolyte membranes on polymeric supports, Langmuir 21 (2005) 10587–10592.
[26] N. Basavegowda, K. Mishra, Y.R. Lee, Ultrasonic-assisted green synthesis of palladium nanoparticles and their nanocatalytic application in multicomponent reaction, New J. Chem. 39 (2015) 972–977.